

Microstructural characteristics of human skin subjected to static *versus* cyclic pressures

Laura E. Edsberg, PhD; Joseph R. Natiella, DDS; Robert E. Baier, PhD, PE; JoAnn Earle, EMT, HT
*Natural and Health Sciences Research Center, Daemen College, Amherst, New York; School of Dental Medicine,
State University of New York at Buffalo, Buffalo, NY; Industry/University Center for Biosurfaces, State University of
New York at Buffalo, Buffalo, NY; Natural and Health Sciences Research Center, Daemen College, Amherst,
New York*

Abstract—Pressure ulcers are generally associated with external pressures exceeding internal capillary pressures over bony prominences when the body cannot initiate motor movement to change positions. This investigation evaluated microstructural changes occurring in human skin, *in vitro*, exposed to static *versus* cyclic pressures, simulating those recorded for heels of human subjects on various pressure-relief mattresses. Morphological data are reported for tissues exposed to pressure in a bench-scale loading system. Dynamic (cyclic-relief) pressure induced parallel alignments of connective tissue collagen bundles, which themselves became differentially oriented to various degrees perpendicular to the surface of the tissue. Static pressure, with no relief, invariably produced alignment of the collagen bundles of the connective tissue parallel to both one another and to the compressed tissue surface. The precursor to pressure ulcer formation may be microstructural alignment in response to the pressure conditions on tissue.

Key words: *bedsore, collagen, decubitus ulcer, elastin, pressure, pressure ulcer, skin.*

INTRODUCTION

This research evaluated the microstructural effects of static *versus* cyclic normal pressures on human skin. Results from the microstructural analyses of control specimens were compared with results for specimens from static and dynamic pressure experimental groups.

Prevention of pressure ulcers might be more effective if the earliest pressure-induced microstructural defects can be identified. Pressure ulcers have been defined simply as “localized areas of cellular necrosis” (1). The etiology of pressure ulcers is multifactorial; however, a major factor is external pressure exceeding internal capillary blood pressure. If capillary blood flow is obstructed for an extended period by such external pressures, one can presume that the resulting ischemia leads to the critical tissue damage that initiates the pressure ulcer (2). There is a reported, inverse relationship between the magnitudes of applied normal-to-surface

This material is based upon work supported by New York State Center for Advanced Technology Health Care Instruments and Devices and the National Science Foundation Industry/University Cooperative Research Center. Both are headquartered at the State University of New York at Buffalo.

Address all correspondence and requests for reprints to Laura E. Edsberg, Natural and Health Sciences Research Center, Daemen College, 4380 Main Street, Amherst, New York 14226; email: LEEedsberg@AOL.com.

forces and the amounts of time required for irreversible tissue damage to occur (3).

Pressure ulcers occur most often over bony prominences covered only by a small amount of muscle and subcutaneous tissue (4,5). The tissue interface “pressure” at such sites is conventionally measured as the normal force applied over the area of the specific sensor; it is seldom explicitly recognized that at a constant force (such as a patient’s own weight), the pressure can significantly increase as the area of actual support decreases. Thus, pressures at bony prominences are high because of the small area over which the force is applied. A “point” force is more damaging to tissue than a force of an identical magnitude over a wider area of the body (4). In addition, the displacement required to reduce oxygen pressure to 0 mmHg is much less over bone than muscle (6).

Sheepskin pads were among the earliest of “devices” used to alleviate pressures at bony prominences. Today, the variety of available devices includes foam pads, air mattresses, water mattresses, fluidized sand beds, perforated air-flow pillows, and alternating-pressure mattresses. Alternating-pressure mattresses were first used in 1948 and continue to be popular (7,8). They employ various geometries of air-filled cells, which inflate and deflate in alternating patterns over cycle times that range from 5 s to 5 min.

Even with the more complex and expensive “pressure-relief” systems, heel pressures remain anomalously high. The heel is particularly sensitive to pressure ulcers because it has no muscle to cushion it and the fat present is minimally vascularized, possibly leading to its rapid breakdown. This anatomic site, of course, is characterized by its sharp bony prominence, presenting a special challenge to pressure-relief systems.

Heel ulcers are considered the most serious. They frequently require amputation of the foot or leg because of complications and infection (9–11), although the incidence of pressure ulcers on the heel is not as high as that on the sacrum (which is the highest incidence). Ulceration of the heel is common in patients with a variety of conditions, including total hip replacements, diabetes, spinal cord injury, stroke, myelodysplasia, or peripheral neuropathy (12). Ulcerations of the heel also frequently lead to infection and osteomyelitis of the calcaneus (12,13).

Several alternative hypotheses exist for the etiology of pressure ulcers, as described by various authors with relevant data. In addition to nominal pressure magnitudes, factors implicated in the etiology of pressure ulcers

have included the nutritional state of the person, metabolic activities, weight, degree of general health, age, the presence of incontinence, moisture, heat, skin surface and subsurface friction, mechanical shear, tissue mobility, presence of infection, neurological damage, and pressure duration (5,7,14–17). Krouskop (18) proposed a model for pressure ulcers based on tissue necrosis initiated by cell-to-cell contact. It is theorized that the cell-to-cell contact occurs when interstitial fluid is disrupted because of an alteration in the capability of the tissue to distribute and support the load. Kosiak (1,19) studied the response of skin to mechanical stress and proposed a pressure-duration relationship for skin breakdown. Daniel (20) found that the initial pathologic changes are seen in muscle tissue when swine are subjected to pressure conditions. As the pressure is increased, or the duration of the pressure is increased, changes are seen in the skin. Several variables can affect the pressure-duration relationship including moisture, shear, nutrition, and friction. Skin structures are altered, depending on the type of mechanical load and duration of the load (21,22).

Several investigators have sought to assess the effects of mechanical stress on skin and tissue using animal models (19,20,23–29). Sanders et al. (21) reviewed the literature, evaluating the response of skin to mechanical stress, and concluded that skin structures adapt and these adaptations depend on the mechanical load direction, duration, and intensity. Goldstein and Sanders (22) used pigs as a model to evaluate adaptation of skin to normal and shear forces and found that tissue adaptation occurred.

Collagen remodeling occurs in normal skin, as a response to stresses and during wound healing (21,30,31). As a result of chronic disease and disability, abnormal loading may occur as a result of paralysis, decreased sensation, and prolonged bedrest or sitting (21). Tissue breakdown occurs as a consequence of the abnormal loads that skin and tissues must bear. Pressure ulcers can occur as a result of this tissue damage (7,18,20,21,32–37).

The precursor to pressure ulcer formation may be microstructural remodeling in response to the pressure conditions on the tissue. Understanding the effects of pressure on the microstructural characteristics of human skin is important for further clarification of the etiology of pressure ulcer formation and the adaptations that tissues undergo. These adaptations may mean the difference between tissue capable of bearing loads and formation of a pressure ulcer. In this study, the effects of pressure on

the microstructural characteristics of human skin are investigated.

MATERIALS AND METHODS

Source of Tissue and Preparation

The foreskin tissue used for the experiments was collected from newborn circumcisions (24–48 h before each experiment) and immediately placed in GIBCO (GIBCO Laboratories, Life Technologies, Inc., Grand Island, NY) keratinocyte media with gentamycin and refrigerated in 50-ml plastic centrifuge tubes. The tissue varied in length from 2 to 3 cm with an average of 2.75 cm and in width from 0.5 to 1 cm with an average of 0.73 cm.

Sensor and Sensor-Gauge Selection

A PSM-1 Pressure Gauge (Gaymar Industries Inc., Orchard Park, NY) and numerous custom-fabricated PSP-1 Pressure Sensors (Gaymar Industries Inc., Orchard Park, NY), designed to be used with this gauge, were employed to measure the tissue interface pressures between the tissue and the watch glass above. PSP-1 pressure sensors are flat flexible polyvinyl chloride plastic envelopes, 2.5 cm × 2.5 cm, with copper contact strips attached diagonally to their opposite inner walls. Air pressure is supplied from the PSM-1 gauge to one end of the otherwise sealed envelope when the cross-oriented copper strips come into contact at their centers and close an electrical circuit. The circuit is connected by wires from the copper strips through the air tube to the gauge. The air supplied from an air pump within the PSM-1 gauge inflates the sensor envelope until a pressure equal and opposite to that closing the sensor is achieved (37). When the internal envelope pressure exceeds the externally applied pressure, the copper strips lose contact and the pump turns off, allowing the pressure to fall until the strips touch and the air pump turns on again (37). This provides “null” pressure readings, where the measuring devices have minimal mechanical interference in the tissue/support-surface interface.

The PSM-1 gauge incorporates a conventional mercury manometer, connected in line with the sensor and the pump, to allow the “null” measurement of tissue interface pressure to be read directly (37). As the “open-close” events of the sensor contact repeat rapidly, the “fluttering” manometer readout typically fluctuates by less than ±2 mmHg. The sensor envelope thickness at this condition is less than 1 mm.

Bench-Top Test Device

Our laboratory designed the bench-top test device to simulate the loading situation at the human heel resting on a mattress or pressure-relief system, but with simplified geometry. Agar was used to simulate the compliant tissue above the bone itself, simulated by a hard spherical section (watch glass). External pressure was applied by another identical watch glass to human skin mounted over the agar layer.

Each tissue specimen was placed on top of agar in its own well of a six-well polystyrene tissue culture plate. Centered within each well bottom, under the agar, was an inverted (convex face up) watch glass of 2.5-cm diameter, which was sealed in place by paraffin around its edge. The watch glass had a radius of curvature of 0.8 cm. Warm agar was poured until it was within 5 mm of the top of each well, providing a pseudo-tissue support matrix layer of 15 mm over the rigid glass. While the agar cooled to 38 °C, the tissue specimens were divided longitudinally, opened, and placed over the centers of the agar zones with their epithelium facing up. The tissue was positioned to maintain dimensions close to those seen *in vivo*, with the use of the rigidity of the agar upon cooling. It is assumed that the dimensions of the positioned tissues reflect some shrinkage as compared to *in vivo* dimensions, because of elastin shrinkage. Liquid nutritional media were added on top of the tissues in each well, and the tissues were kept moist and alive throughout the experiment. As the agar then cooled further, it secured the tissue in place over the agar/watch glass combination, simulating an anatomical bony prominence.

The skin was contacted from above by the convex face of an identical 2.5-cm-diameter watch glass. This was accomplished by use of the top of a six-well tissue culture dish having plastic mounts (50-ml centrifuge tube lids) cemented to its surface (see **Figure 1**). Since the watch glasses were smaller in diameter than the wells, they fit easily.

Both static and cyclic normal pressures were applied to human epidermis with the use of a bench-top loading system. A small motor was used to raise and lower the lid of the tissue culture dish to provide cyclic pressures to the tissues (**Figure 1**). Clamps held the lid and well plate combinations, described above, in constant registry. Raising the lid decreased the maximum interface pressure, while lowering the lid increased it. Cyclic pressure was applied as 20 compressions and lifts per minute, with pressure constant for 2 s/cycle. Continuing static pressure was applied by adjusting the height of the lid to the

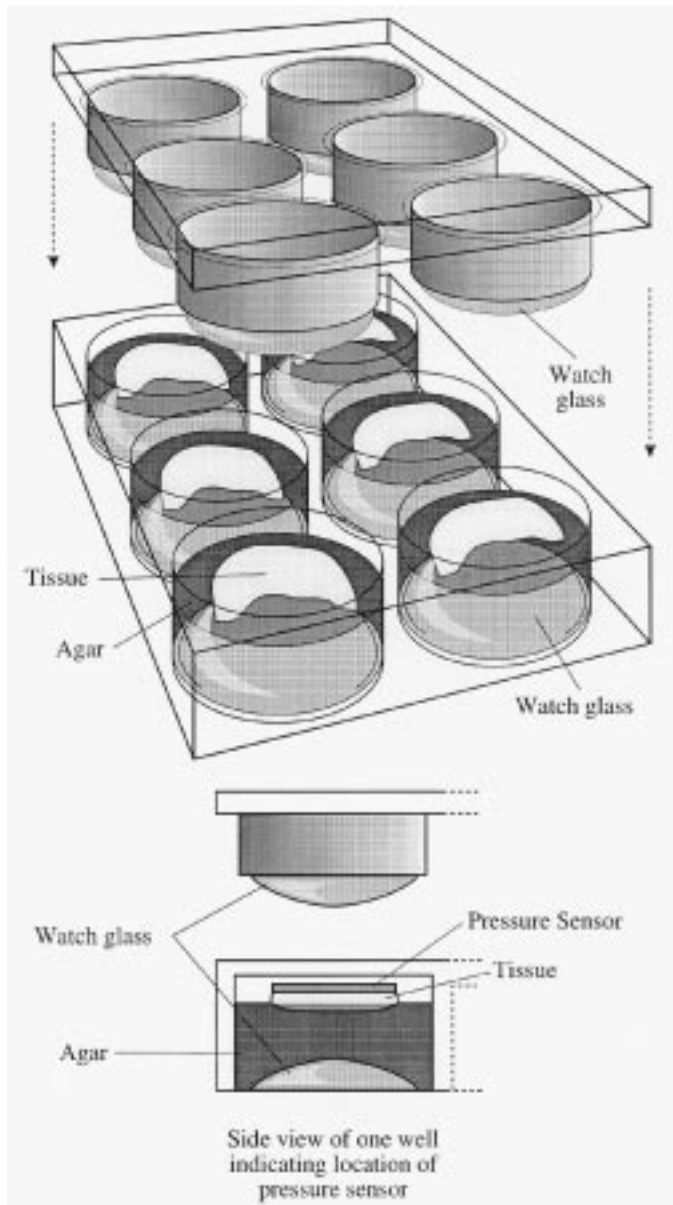


Figure 1.
Bench-Top Model.

desired loading and holding the lid at that position and pressure until the end of the experiment. Pressure sensors and gauge combinations were incorporated in each experiment to monitor the pressure applied to the tissues. Sensors were placed in each well between the tissue, and the corresponding watch glass was attached to the lid. The interface pressure was monitored for each well in the plate. The tissues were kept at 37 °C during the experiments.

The bench-top model experiments included these static and dynamic pressure groups: 50 mmHg (6.7 kPa) and

170 mmHg (22.7 kPa) static normal pressure and dynamic normal pressure cycled between 110 to 170 mmHg (14.7 kPa to 22.7 kPa). These groups were chosen based on prior experiments that used human subjects resting on pressure-relief systems. The three pressure groups represent average values recorded from the prior studies (38). All the group values were recorded by the same sensors used throughout this and prior investigations. At least three separate human tissue specimens, from different donors, were subjected to each of these conditions. Control specimens were also from different donors. The control specimens were placed in the bench-top test device, but were not subjected to compressive loading.

Before histological evaluation, each tissue specimen was subjected to one of three compressive loading conditions with the use of the bench-top device. After each 4-h experiment, the tissues were removed from their agar supports and immediately fixed in 10-percent buffered formalin at room temperature for a minimum of 36 h before the tissue was dehydrated, embedded, sectioned, and stained for structural examination at the light-microscopic level. The choice of 4-h experimental periods was based on results from a pilot study, done first to examine the microstructural integrity of isolated (unpressurized) skin after 4, 8, 12, 16, 20, 24, 28, and 32 h on agar with media at room temperature. The results of these pilot studies indicated that considerably more than 4 h was required before noticeable microstructural changes spontaneously appeared.

Histological Processing

The histological evaluation of each tissue specimen began by processing and embedding the tissue in paraffin. Both the control and experimental specimens were embedded and sectioned at the same orientations. Cross sections of 5 μ m of the tissue in blocks of paraffin were sliced with a microtome. The glass slide mounted sections were then stained with 5–10 replicates for each of the three stains. The stains used were hematoxylin and eosin (H&E), Masson's trichrome, and Verhoeff's stain. Sections stained with hematoxylin and eosin have nuclei that were stained blue, cartilage and calcium deposits stained dark blue, cytoplasm and other constituents stained shades of red, and blood stained bright red. Masson's trichrome were stained nuclei black, while cytoplasm, keratin, and muscle fibers were stained red. Collagen and mucin were stained blue. Verhoeff's stain made elastic fibers blue-black to black. Nuclei were stained blue to black and collagen stained red. Other tissue elements were stained yellow.

Classification of Response Component of Models

A minimum of five and a maximum of ten sections were analyzed for each of the three separate tissue specimens, for each set of conditions. Using comparisons between control and experimental sections, the blinded evaluator analyzed these sections. A blinded pathologist, grading epithelial configuration and morphologic changes in dermal components, divided the responses at the test site into minimal or maximum response.

Epithelium Configuration

Minimal Response: preservation of original papillary surface elevations, with maintenance of original epithelial thickness.

Maximum Response: flattening of original surface elevations, with thinning (compression of the epithelial thickness) to less than two-thirds initial thickness.

Dermal Components

Minimal Response: preservation of the initial vascular components with easy determination of luminal outlines, maintenance of original fiber bundle orientation and staining quality, and identification of elastic fiber grouping using special staining.

Maximum Response: sufficient compression of small blood vessels to obscure luminal diameters, concurrent compression of fiber bundle components as revealed by opaque staining, and poor delineation of elastic fibers and/or interruption of grouping.

RESULTS

Histomorphology of Control Test Sites

The human foreskin tissue site tested is composed of fibroelastic tissue, which is surfaced by orthokeratinized stratified squamous epithelium. The surface has an undulating configuration, a feature resulting from the presence of high dermal papillae. Narrower zones of elevation have features that resemble papillomatous folds. The outer orthokeratin, which surfaces the epithelium, is firmly adherent following sectioning. There is a vividly staining stratum granulosum rich in keratohyaline granules. The deeper stratum spinosum has a highly variable thickness that, in some areas, ranges from five to eight cell layers. Thicknesses of three to five cells predominate. Within the stratum spinosum, individual cells have indistinct cytoplasmic boundaries without prominent cell membrane detail. The nuclei are ovoid basophilic struc-

tures, often bordered by narrow clear zones of cytoplasm. Nucleoli are faint and vary from one to three in number. The basal layer nuclei have dense basophilia, and this deepest layer of epidermis is a sharp delineation from the overlying stratum spinosum. The stratum basalis has a one- to four-cell layer thickness. Mitotic division is rare. Many specimens demonstrate basal layer cells with an ovoid shape and cytoplasm with melanin granules. Some ridges are "saw toothed," while others are blunted and fused. Still others are flat. Flattened ridges are often associated with invaginations of the surface and plugs of orthokeratin.

The basement membrane zone is narrow and indistinct and is delineated only by a broad amorphous band of staining. The underlying connective tissue is intermediate between loose and dense, therefore designated as "moderately dense." Fiber bundles are best characterized in modified Masson stained sections and appeared short with indistinct cytoplasmic boundaries. Scattered nuclei have both blunted and stellate forms. The connective tissue has lesser density within the dermal papillae. An easily separated papillary/reticular dermis is not readily apparent, but a merging of thin short fiber bundles occurs with broad and long fiber bundles in the deep dermis. Elastic stains confirm this general pattern. Subjacent to the epidermis, there are short elastin fibers with a multidirectional arrangement and some condensation around small blood vessels. Deeper regions of the connective tissue have broader and longer elastin fibers (see **Figure 2a, b, c, d**).

The connective tissue zone subjacent to the epidermis was richly vascularized. Delicate endothelial-lined channels possessed varied caliber and length. This was an impressive feature of the foreskin, with cavernous-like endothelial-lined channels extending to the actual base of many specimens. The test tissue did not possess skin appendage structures. Occasional rare sebaceous glands were seen. Portions of the keratinocytes have cytoplasmic clear zones; this is a combined factor of staining and fixation after a period of experimental analysis. This appears primarily in the spinous zone, and intercellular vacuolization indicating severe tissue damage is not seen.

Microstructural Findings After Bench-Top Compression

The histomorphology of human foreskin tissue specimens subjected to 50-mmHg static sensor pressure was as follows: The test sites showed minimal alteration of epidermal structures and connective tissue. There was preservation of surface elevations with retention of the

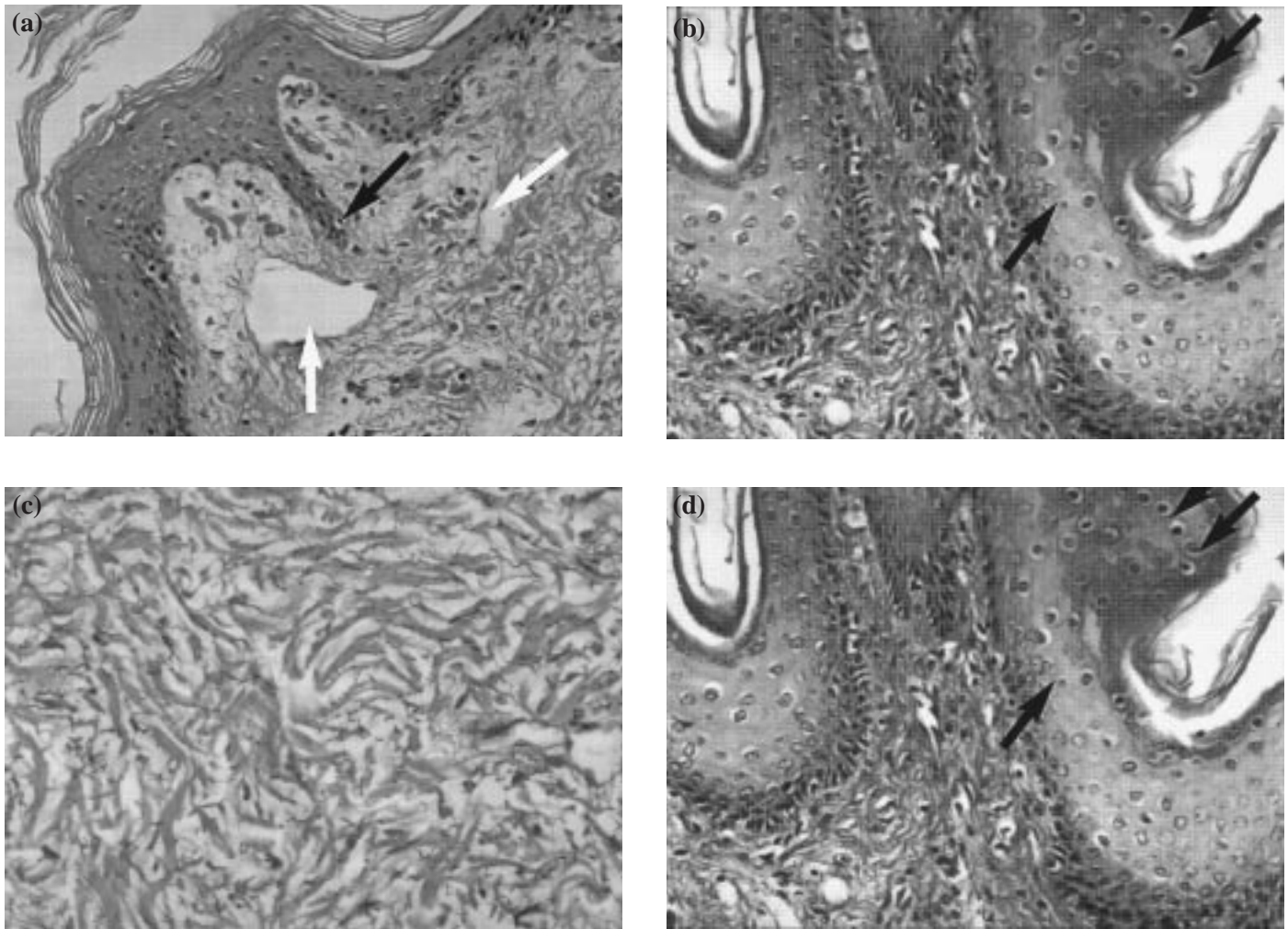


Figure 2.

Human Foreskin Tissue. *Masson's Stain*, 250 \times : (a) Properties of test site epidermis and underlying connective tissue are shown. Some rete ridges are saw-toothed (black arrow); others are flattened with depressions containing bands of orthokeratin. Abundant vascular component (white arrows) can be appreciated with a wide range of luminal caliber. Here, connective tissue is looser and more faintly staining than in deeper zones of foreskin. (b) A comparatively thick epidermis surfaces this area of test site. At this magnification, faintly basophilic ovoid nuclei with clear cytoplasmic boundaries are well-detailed (black arrows). *Verhoeff's Stain*, 400 \times : (c) Elastic connective tissue component of superficial connective tissue consists of small strands of elastin. Zone between dermal papillae and base areas of test site shows dark-staining short elastin fibers with a multidirectional fiber array. *Verhoeff's Stain*, 1000 \times : (d) Deeper segments of test site show broad and long elastin fibers (black arrows). Note also fibronuclei with both blunted and stellate shapes.

outer keratin layer. There was no alteration of the multidirectional configuration of the fiber bundles in the superficial or deeper dermis. It was significant that elastin fibers remained easily delineated from surrounding structures (see **Figure 3a, b**). The epithelial/connective tissue junction remained intact and individual epithelial cell relationships were maintained. Within the connective tissue, small endothelial-lined channels were readily identified with lumen diameters that were similar to those of control sections.

In contrast, similar specimens examined after being subjected to 170-mmHg static sensor pressure did exhibit significant alteration from normal structure as compared against control sections. The surface of the tissue was flattened and the rete ridge configuration was blunted. Fiber bundles showed a layered appearance with reduction of the lumens of small capillaries. Especially notable was the fact that elastic fibers, although remaining visible, now showed an alignment parallel to that of the collagen fiber bundle arrangement (see **Figure 4a, b**).

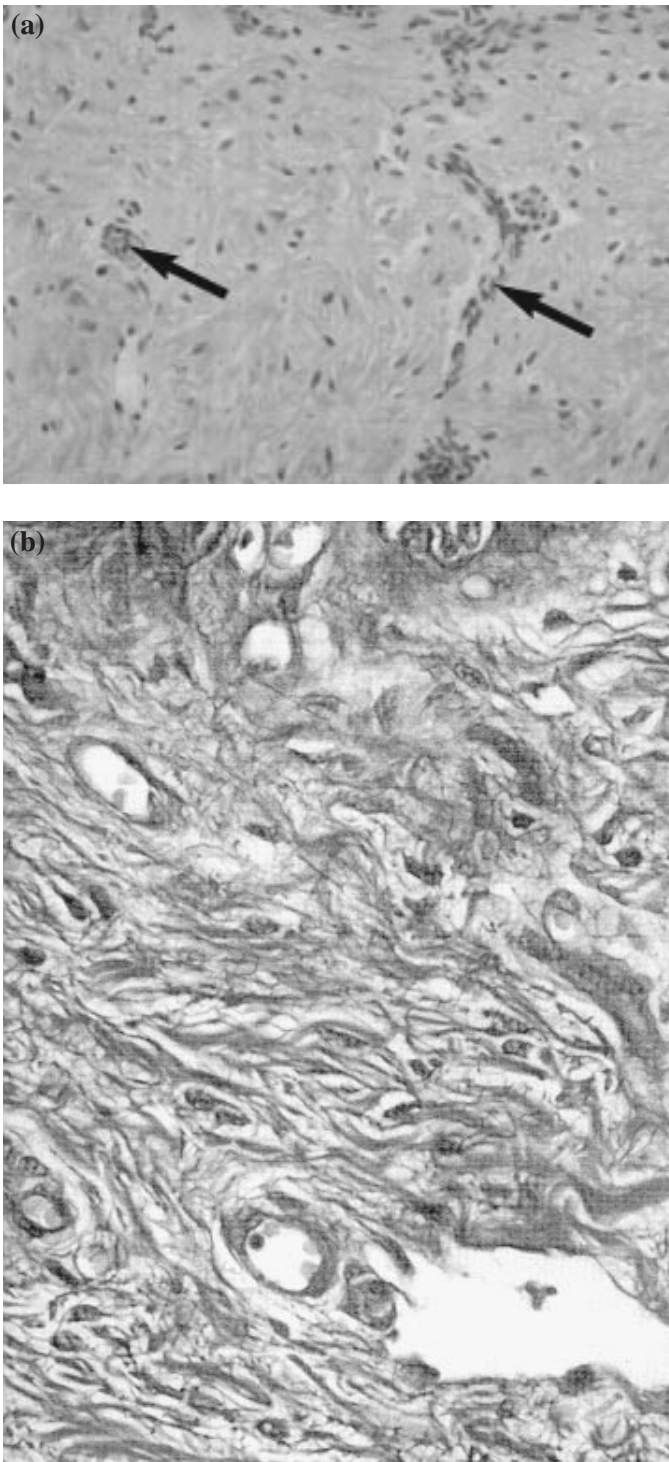


Figure 3. Human Foreskin Tissue, Bench-top Model Experimental 50-mmHg Static Pressure. *H & E Stain*, 250 \times : (a) Multidirectional orientations of superficial and deep dermis are illustrated, as are well-delineated capillaries of varied caliber (black arrows). *Verhoeff's Stain*, 400 \times : (b) Interposed with superficial layer fiber bundles are small elastin fibers with same prominence observed in control sections.

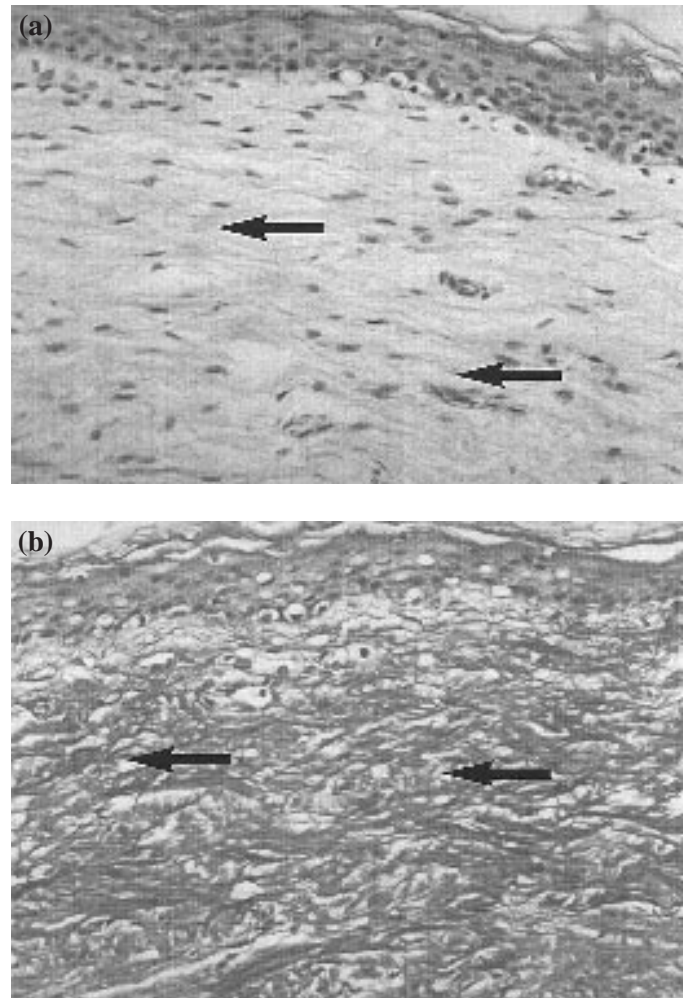


Figure 4. Human Foreskin Tissue, Bench-top Model Experimental 170-mmHg Static Pressure. *H & E Stain*, 250 \times : (a) Surface appears flattened and keratin exhibits fragmentation. At this magnification, parallel arrangement (black arrows) of fiber bundles in superficial dermis is readily seen. *Masson's Stain*, 250 \times : (b) This photomicrograph shows parallel arrangement (black arrows) of connective tissue fibers in superficial dermis.

The underlying connective tissue showed additional evidence of surface compression. There was some fragmentation of the overlying orthokeratin although this was difficult to quantitate in relation to some sectioning artifact. The bordering segments of most specimens retained their papillary features.

Specimens examined following 110–170 mmHg of dynamic (cyclic) sensor pressure exhibited only minimal alteration of epithelial and connective tissue components. The original surface topography was preserved. Changes noted consisted of a parallel orientation of some fiber bundles and formation of “tuft-like” structures within the epi-

dermal ridges. Elastin fibers were more visible in these areas, which showed parallel orientations of small blood vessels at right angles to the surface. Elsewhere, the superficial connective tissue zone contained small, less distinct elastin fibers that more closely resembled control sections than static-compressed sections (see **Figure 5a, b**).

DISCUSSION

Prior studies of pressure-relief systems show that most allow interface pressures considerably greater than 32 mmHg (4.3 kPa) and some dynamic systems, even when deflated, may sustain these adverse interface pressures (38). Dynamic systems, when inflated, typically elevate tissue interface pressures to appreciably greater values than found on static pressure-relief systems, but when deflated, usually have considerably lower pressures than static systems. Since the dynamic systems provide pressures both greater than and less than those of the static systems, it is relevant to compare the microstructural changes seen for both static and dynamic systems.

This study simulated the clinically important pressure-induced microstructural damage of static and cyclic loads on skin, with the use of a bench-scale system designed to apply either static or cyclic normal pressures in a circular, symmetrical fashion. With the use of healthy newborn tissue, experimental conditions (pressure applications) selected from prior human subject trials produced microstructural changes after 4 h of pressure application, and these changes were readily differentiated from unrelated (e.g., autolytic) degradation of the tissue over that time. The pressures used for the bench-top experiments were always greater than the presumed minimum capillary closing pressure and within the range of pressures actually produced by commercial clinical pressure-relief systems at the heels of human subjects in previous experiments.

The skin used in our study did not have a blood supply present during the experiment. Thus, the changes studied were a result of the loading conditions only. Without perfusion present, the bench-scale loading system represents tissue in a severely ischemic environment. The results of this research suggest the need to study further both the microstructural and biochemical effects of abnormal loading on tissue *in vivo*.

Implications for Better Prevention of Pressure Ulcers

As these histologic results show, pressure may have a significant characteristic effect on the microstructure of

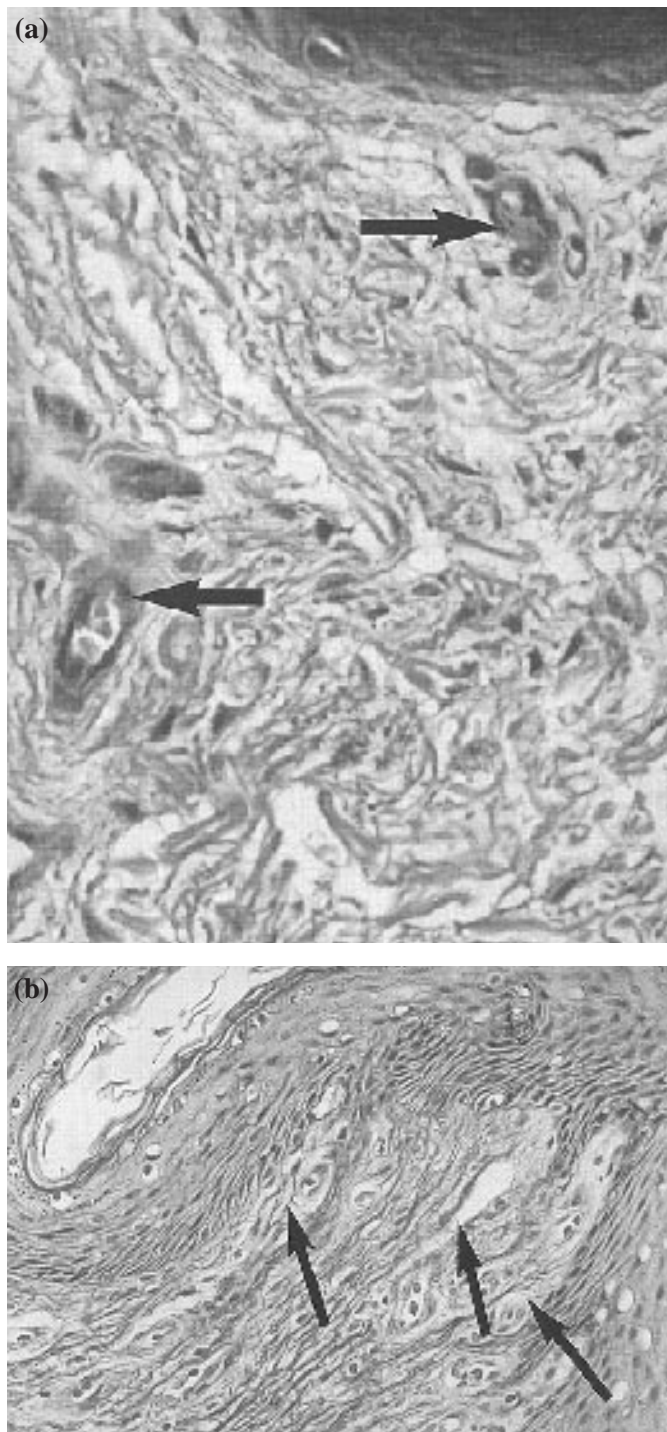


Figure 5.

Human Foreskin Tissue, Bench-Top Model Experimental 110- to 170-mmHg Dynamic (cyclic) Sensor Pressure. *Verhoeff's Stain*, 250 \times : (a) Special stain illustrates even spacing between fiber bundle components and prominent vascular lumens (black arrows). *Masson's Stain*, 250 \times : (b) Experimental condition produced "tuft-like" dermal papillae (black arrows), with elongation of capillary component at right angles to surface.

skin and on the orientation of dermal collagen fiber bundles, in particular. The alignment of the connective tissue bundles parallel to one another and parallel (or perpendicular) to the compressed surface might well indicate the beginning of matrix breakdown, which can then lead to the formation of pressure ulcers.

The bench-top model tissue groups subjected to 170-mmHg static sensor pressure and 110- to 170-mmHg dynamic sensor pressure showed significant early (4 h) microstructural changes. These may be of direct relevance in initiation of pressure ulcer formation. The 170-mmHg static sensor pressure group showed collagen fiber bundles and elastic fibers in parallel alignment and oriented parallel to the loaded tissue surface. The tissue subjected to 110- to 170-mmHg dynamic sensor pressure had an elongated capillary component. Fiber bundles paralleled these blood vessels, but both components were oriented perpendicular to the original tissue surface. Surface undulations of the tissue epidermal zone also were retained better by tissue subjected to dynamic pressure.

The function of skin microstructure in the development of pressure ulcers has been largely overlooked. Crenshaw and Vistnes (39) have shown that skin necrosis starts in the dermis where collagen is located, and Krouskop (18) has suggested a model in which a network of collagen and elastin fibers work to transmit loads between the skin and skeletal surface. Goldstein and Sanders (21,22) have sought to characterize the relationship between mechanical stress and the correlated changes seen in the tissue. Doillon et al. (40) found that the mechanical properties of wound tissue are related to the orientation, fiber diameter, volume fraction, and composition of the collagen involved. Doillon et al. (41) reported that tensile failure of a wound was caused by the failure of the architecture of the collagen bundles to support the mechanical load.

Although all the presently reported experiments were conducted on healthy neonatal tissue, these findings indicate a significant realignment of the collagen bundles of connective tissue and thus have very serious implications in regards to the capability of the tissue to sustain potentially damaging mechanical loads. Human foreskin tissue differs from the heel region in that the skin is not as thick or calloused, but both tissues are from regions with little fat present. The epidermal thickness of both tissues is similar. It is expected that similar experiments with elderly, debilitated, or other populations at greater risk for pressure ulcer formation would show even more profound realignments.

Currently, studies are underway in our laboratory to morphometrically, mechanically, and biochemically eval-

uate tissue at and adjacent to pressure ulcers in human patients.

ACKNOWLEDGMENT

The research was performed at Biomedical Research Laboratory, Sisters of Charity Hospital, 2157 Main Street, Buffalo, NY 14214.

REFERENCES

1. Kosiak M. Etiology of decubitus ulcers. *Arch Phys Med Rehabil* 1961;42:19-29.
2. Krouskop TA, Noble PC, Garber SL, Spencer WA. The effectiveness of preventative management in reducing the occurrence of pressure sores. *J Rehabil Res Dev* 1983;20:74-83.
3. Brand PW. Pressure sores—The problem. *Bedsore Biomechanics*. Baltimore, MD: University Park Press. 1976;19-23.
4. Husain T. An experimental study of some pressure effects on tissues, with reference to the bed-sore problem. *J Pathol Bacteriol* 1953;66:347-58.
5. Kosiak M. Etiology and pathology of ischemic ulcers. *Arch Phys Med Rehabil* 1959;40:62-9.
6. Sangeorzan B, Harrington R, Wyss C, Czernieki J, Matsen F. Circulatory and mechanical response of skin to loading. *J Orthoped Res* 1989;7:425.
7. Yarkony GM. Pressure ulcers: a review. *Arch Phys Med Rehabil* 1994;75: 908-17.
8. Berecek KH. Treatment of decubitus ulcers. *Nurs Clin North Am* 1975;10:171-210.
9. Kataria MS, Datta AK. Management of pressure areas in the elderly. *Practitioner* 1982;226:1174-7.
10. Hendricks, WM. Pressure ulcers (letter). *Ann Intern Med* 1981;95:239.
11. Versluisen M. Pressure sores in elderly patients: The epidemiology related to hip operations. *J Bone Joint Surg Br* 1985; 67(B#1):10-3.
12. Crandall RC, Wagner FW. Partial and total calcaneotomy. *J Bone Joint Surg Am* 1981;63(A):152-5.
13. Sugarman B, Hawes S, Musher DM, Klima M, Young EJ, Pircher F. Osteomyelitis beneath pressure sores. *Arch Intern Med* 1983;143:683-8.
14. Berjian RA, Douglass HO, Holyoke ED, Goodwin PM, Priore RL. Skin pressure on various mattress surfaces in cancer patients. *Am J Phys Med* 1983;62:217-26.
15. Elliot TM. Pressure ulcerations. *Am Fam Physician* 1982;25:171-80.
16. Longe RL. Current concepts in clinical therapeutics: pressure sores. *Clin Pharmacy* 1986;5:669-81.
17. Crenshaw RP, Vistnes LM. A decade of pressure sore research: 1977-1987. *J Rehabil Res Dev* 1989;26(1):63-74.
18. Krouskop TA. A synthesis of the factors that contribute to pressure sore formation. *Medical Hypotheses* 1983;11:255-67.

19. Kosiak M. Etiology and pathology of ischemic ulcers. *Arch Phys Med Rehabil* 1959;40:62-9.
20. Daniel RK, Priest DL, Wheatley DC. Etiologic factors in pressure sores: an experimental model. *Arch Phys Med Rehabil* 1981; 62:492-8.
21. Sanders JE, Goldstein BS, Leotta DF. Skin response to mechanical stress: adaptation rather than breakdown. A review of the literature. *J Rehabil Res Dev* 1995;32(3):214-26.
22. Goldstein B, Sanders J. Skin response to repetitive mechanical stress: a new experimental model in pig. *Arch Phys Med Rehabil* 1998;79:265-72.
23. Dinsdale SM. Decubitus ulcers in swine: light and electron microscopy study of pathogenesis. *Arch Phys Med Rehabil* 1973;54:51-7.
24. Manley MT, Darby T. Repetitive mechanical stress and denervation in plantar ulcer pathogenesis in rats. *Arch Phys Med Rehabil* 1980;61:171-7.
25. Husain T. An experimental study of some pressure effects on tissues, with reference to the bed-sore problem. *J Pathol Bacteriol* 1953;66:347-58.
26. Lindan O, Greenway RM, Piazza JM. Pressure distribution on the surface of the human body: I. Evaluation in lying and sitting positions using a "bed of springs and nails." *Arch Phys Med Rehabil* 1965;46:378-85.
27. Kosiak M. Etiology of decubitus ulcers. *Arch Phys Med Rehabil* 1961;42:19-29.
28. Barton AA, Barton M. Plantar ulcers occurring after neurectomy: a light and electron microscope study. *Aust J Exp Biol Med Sci* 1968;46:155-63.
29. Goldstein B, Sanders J. Skin response to repetitive mechanical stress: a new experimental model in pig. *Arch Phys Med Rehabil* 1998;79:265-72.
30. Craig AS, Eikenberry EF, Parry DAD. Ultrastructural organization of skin: classification on the basis of mechanical role. *Connect Tiss Res* 1987; 16:213-23.
31. Moore JC, Ray AK, Shakespeare PG. Surface ultrastructure of human dermis and wounds. *Br J Plast Surg* 1993;46:460-5.
32. Krouskop TA, Reddy NP, Spencer WA, Secor JW. Mechanisms of decubitus ulcer formation—An hypothesis. *Medical Hypotheses* 1978;4:37-9.
33. Reddy NP, Cochran GVB, Krouskop TA. Technical note: interstitial fluid flow as a factor in decubitus ulcer formation. *J Biomech* 1981;14(12):879-81.
34. Reuler JB, Cooney TG. The pressure sore: pathophysiology and principles of management. *Ann Int Med* 1981; 94:661-6.
35. Rodriguez GP, Murphy KP. Current trends in pressure ulcer research. *Crit Rev Phys Rehabil Med* 1996; 8(1&2):1-18.
36. Rudd TN. The pathogenesis of decubitus ulcers. *J Am Geriatr Soc* 1962;10:48-53.
37. Stewart TP. Use of the Gaymar pressure gauge and electropneumatic sensor. Technical Report. Orchard Park, NY: Department of Medical Research, Gaymar Industries, Inc.; 1984.
38. Edsberg LE. Comparative measurements of interfacial pressures between tissue sites and various support systems [master of science thesis]. Buffalo, NY: State University of New York at Buffalo; 1992.
39. Crenshaw R, Vistnes L. A decade of pressure sore research. *J Rehabil Res Dev* 1989;26:1.
40. Doillon CJ, Silver FH, Olson RM, Kamath CY, Berg RA. Fibroblast and epidermal cell-type I collagen interactions: cell culture and human studies. *Scan Microsc* 1988; 2(2):985-92.
41. Doillon CJ, Dunn MG, Bender E, Silver FH. Collagen fiber formation in repair tissue: development of strength and toughness. *Collagen Rel Res* 1985;5:481-92.

Submitted for publication July 10, 1998. Accepted in revised form April 27, 1999.